

Continuous-wave measurement of the hydrogen 1S-2S transition frequency

D. H. McIntyre,* R. G. Beausoleil,[†] C. J. Foot,[‡] E. A. Hildum,[§]
B. Couillaud,** and T. W. Hänsch^{††}

Department of Physics, Stanford University, Stanford, California 94305

(Received 3 February 1988; revised manuscript received 14 November 1988)

We have measured the 1S-2S transition frequency in atomic hydrogen with a precision of 7 parts in 10^{10} by continuous-wave Doppler-free two-photon spectroscopy. We employ cavity-enhanced multimilliwatt radiation near 243 nm produced by sum-frequency generation, and we observe the 1S-2S transition in a low-pressure hydrogen-helium cell with a resolution of 3 parts in 10^9 . For a frequency comparison we detect an optical heterodyne signal at the difference frequency between the 243-nm light used to excite the 1S-2S transition and the second harmonic of a reference laser locked to an interferometrically calibrated $^{130}\text{Te}_2$ absorption line near 486 nm. After determining systematic corrections due to the pressure shift of the $F=1$ hyperfine component in a 0.7 vol. % hydrogen-99.3 vol. % helium gaseous mixture, we obtain the energy-level separation $f(1S-2S) = 2\,466\,061\,413.2(18)$ MHz. Choosing a value of the Rydberg constant measured independently by high-resolution spectroscopy of the hydrogen Balmer- β transition, we find the hydrogen ground-state Lamb shift to be $f_{LS}(1S) = 8173.9(19)$ MHz, in good agreement with the theoretical value of 8172.89(9) MHz.

I. INTRODUCTION

Precision spectroscopy of one-electron atoms has played a central role in the development of quantum electrodynamics (QED). In particular, increasingly refined microwave spectroscopic measurements of the $2S_{1/2}-2P_{1/2}$ Lamb shift have inspired much of the progress made in QED calculations of hydrogen energy levels, which can be performed very accurately due to the extreme simplicity of the hydrogen atom. The most recently published measurements of this Lamb shift are due to Lundeen and Pipkin,¹ 1057.845(9) MHz, and Pal'chikov, Sokolov, and Yakovlev,² 1057.8514(19) MHz, and are in good agreement with the calculated value of 1057.849(11) MHz.^{3,4} Eventually, however, the accuracy with which this number can be experimentally determined must be limited by the 1.6-ns lifetime of the $2P$ state. Since the result of Pal'chikov *et al.* already has an uncertainty of only 2 parts in 10^5 of the 100-MHz natural linewidth of the $2S_{1/2}-2P_{1/2}$ transition, significant improvement in this measurement may be difficult to achieve.

Instead, the $1S_{1/2}-2S_{1/2}$ transition (hereafter simply referred to as the 1S-2S transition) in atomic hydrogen⁵⁻¹¹ may someday offer the ultimate confrontation between the theory of bound-state QED and the experimental techniques of high-resolution laser spectroscopy. Because the Lamb shift of a particular state is proportional to the square of the electron wave function at the nucleus, it scales as $1/n^3$, so that the shift of the 1S level is eight times larger than that of the 2S level. Also, since the lifetime of the metastable 2S state is limited only by spontaneous two-photon emission to the 1S state, the 1S-2S transition has an unusually narrow natural linewidth of 1.3 Hz, offering an eventual experimental resolution of 5 parts in 10^{16} . Consequently, a measurement of the ab-

solute frequency of this fundamental transition and comparison with other hydrogen transitions could provide a stringent test of the low-energy behavior of QED.

As a step towards this goal, we have used continuous-wave (cw) Doppler-free two-photon spectroscopy to observe the 1S-2S transition in atomic hydrogen gas with a resolution of 3 parts in 10^9 . This has allowed us to measure the frequency of this fundamental transition with a precision of 7 parts in 10^{10} , and as a result, we have been able to determine the 1S Lamb shift to within 2 parts in 10^4 .

II. EXPERIMENTAL APPARATUS

A schematic diagram of the entire hydrogen 1S-2S experiment is shown in Fig. 1. There are four major components: (1) the 243-nm sum-frequency synthesizer,⁴ (2) the hydrogen 1S-2S spectrometer,⁴ (3) the 486-nm tellurium optical frequency standard, and (4) the optical heterodyne system for frequency comparison.

Continuous-wave 243-nm radiation is generated by efficient 90° phase-matched sum-frequency mixing of a 790-nm ring dye laser (Coherent 699-21) and a 351-nm argon-ion laser in a potassium dihydrogen phosphate (KDP) crystal heated to 62°C . The 790-nm fundamental beam is enhanced using a servo-locked passive ring cavity. This enhancement cavity closely resembles the ring dye laser resonator and is stabilized to the 790-nm laser frequency with the polarization stabilization scheme of Hänsch and Couillaud.¹² We routinely obtain enhancement of 60-70 of the 500-600 mW of input power. The principles behind the design of the 790-nm enhancement cavity are well known.¹³⁻¹⁷

Approximately 500-800 mW of narrow-band cw 351-nm fundamental laser radiation is provided by an argon-

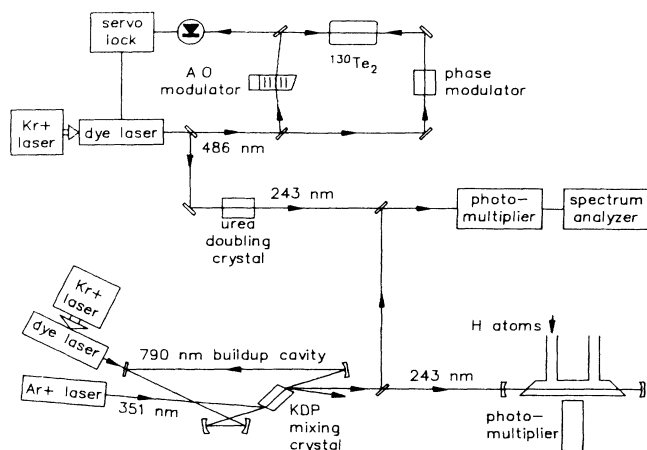


FIG. 1. Schematic diagram of hydrogen 1S-2S experiment. AO modulator is acousto-optic modulator.

ion laser (Coherent I-100) with a prism wavelength selector and an uncoated fused quartz intracavity etalon to force single-frequency operation.¹² The argon-ion laser is servo locked to a temperature-stabilized, passive reference étalon in much the same way as the dye laser.

Our KDP crystal is 45° z cut, has a volume of 25×8×8 mm³, and has faces at Brewster's angle. We achieve type I, 90° phase matching by varying the temperature in the crystal.¹⁸ The radius of the 790-nm beam waist within the KDP crystal, 40 μm, is about 5 μm larger than the value which is expected to maximize the sum-frequency output.^{10,19} We are able to generate 3–5 mW of 243-nm light under favorable fundamental beam conditions.

The 243-nm radiation is mode matched into a servo-locked standing-wave cavity that surrounds the excitation and observation region. The ultraviolet light is enhanced by a factor of 8–16 and the cavity is stabilized with the method of Hänsch and Couillaud¹⁷ by analyzing the polarization of the light reflected from the outer surface of one of the Brewster windows.

Hydrogen atoms in the ground state are produced by 2.45-GHz microwave dissociation of molecular hydrogen in a flowing gas discharge. Atoms leave the discharge through a small constriction and are transported to the observation cell by a length of Teflon tubing. The cell is made of Pyrex and the pressure in the cell is measured with a Baratron gauge. The discharge is typically run with a pressure of several Torr which produces a cell pressure of less than 1 Torr. The discharge is operated alternately with 100% H₂ and a 0.7 vol. % H₂–99.3 vol. % He mixture in order to investigate the pressure shift and broadening of the 1S-2S transition. The resonance signal is detected by counting Lyman-α photons emitted when excited 2S atoms are collisionally transferred to the 2P_{1/2} state. The fractional solid angle of the photomultiplier is 2.5×10⁻³ and the total detection efficiency is 4×10⁻⁵.

III. FREQUENCY STANDARD

Our optical frequency standard is a Doppler-free transition in molecular tellurium vapor (¹³⁰Te₂) near 486 nm.

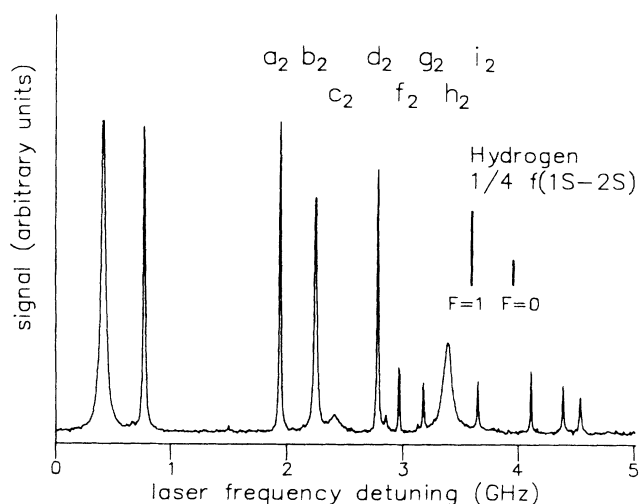


FIG. 2. Doppler-free spectrum of ¹³⁰Te₂ at 486 nm in the vicinity of the hydrogen 1S-2S reference line *i*₂. Also shown are the expected locations (at 486 nm) of the two hyperfine components of the hydrogen 1S-2S transition.

This reference line, shown in the Doppler-free saturated-absorption spectrum of Fig. 2, is labeled *i*₂ and is a component of the Doppler-broadened line labeled No. 1286 in the ¹³⁰Te₂ atlas²⁰ at 20 564.7181(20) cm⁻¹. The isotopically pure (≈99%) ¹³⁰Te₂ is contained in a sealed cell which is maintained at a temperature of 513(5)°C, corresponding to a tellurium vapor pressure of 0.89(11) Torr.²¹ At this temperature, the single-pass linear absorption on a Doppler-broadened line (No. 1284 in the ¹³⁰Te₂ atlas) 10 GHz below the *i*₂ component is 23(2)%. The tellurium transition is excited with an additional cw ring dye laser operated with coumarin 102 dye.

The frequency of the *i*₂ reference line is determined from two separate interferometric measurements. In the first, the frequency of the *i*₂ line is measured with respect to the nearby *b*₂ line, which was previously calibrated by Barr *et al.*²² by comparison with an iodine stabilized helium-neon laser at 633 nm. The *i*₂–*b*₂ frequency separation is only 1.4 GHz and is measured in the same fashion as a previous measurement of another ¹³⁰Te₂ reference line.²³ The uncertainties in this determination are shown in Table I and the result is shown as the first

TABLE I. Frequency measurement uncertainties of the ¹³⁰Te₂ *i*₂ component from its calibration with respect to the *b*₂ component.

Source of uncertainty	Error ^a (MHz)
Statistical	0.05
Computer fitting	0.19
Pressure shift	0.17
<i>b</i> ₂ reference line ^b	0.25
Irreproducibility	0.34
Total	0.50

^aOne standard deviation.

^bReference 22.

TABLE II. Frequency measurements of the $^{130}\text{Te}_2$ i_2 reference line.

	Frequency (MHz)	Error ^a (MHz)
i_2 referenced to $^{130}\text{Te}_2$ b_2 component	616 515 332.88	0.50
i_2 referenced to three $^{127}\text{I}_2$ lines	616 515 332.58	0.56
i_2 weighted average	616 515 332.75	0.39

^aOne standard deviation.

entry in Table II. The measurement uncertainties include a 0.34-MHz uncertainty due to the irreproducibility of tellurium reference lines, since our cell has not been directly compared with the cell used by Barr *et al.* The cells are nominally identical, having been obtained from the same source. We have estimated this irreproducibility uncertainty from data obtained with a second parallel $^{130}\text{Te}_2$ saturation spectrometer,^{23–25} as well as data from an absolute frequency measurement of tellurium transitions in our primary cell (see Ref. 25 and below). The 0.34-MHz uncertainty is the simple average of the absolute values of measured differences (eight total comparisons) for five transitions (i_2, b_2, b_1, e_3, d_4 components) in four different cells (three in our lab and the one of Barr *et al.*).^{22–25}

In a second experiment the frequency of the i_2 reference line was interferometrically measured with respect to three high-precision iodine transitions at 515 nm, 576 nm, and 612 nm. These transitions are among those recommended for realization of the new definition of the meter.²⁶ The result of that measurement (details will be published separately) is shown as the second entry in Table II, where its large uncertainty is mainly due to larger systematic uncertainties associated with the interferometric technique. These two results can then be combined to yield the result shown in Table II, where we have assumed that 0.16 MHz of the systematic errors are correlated, since both measurements were performed in the same cell under similar conditions.

To use the i_2 transition as a frequency standard in the 1S-2S measurement, the 486-nm dye laser is stabilized to the transition using the technique of frequency-modulation spectroscopy.^{27,28} The frequency of the stabilized laser is determined as shown in Table III. We use an angle-tuned urea crystal²⁹ to generate approximately 1

TABLE III. Frequency determination of 486-nm reference laser.

Term	Frequency (MHz)	Error ^a (MHz)
$^{130}\text{Te}_2$ i_2 component frequency	616 515 332.75	0.39
Acousto-optic shift	−60.00	0.00
FM signal offset	−0.03	0.05
Lock-point offset	0.06	0.01
Reference laser frequency	616 515 272.78	0.39

^aOne standard deviation.

nW of the second harmonic of the stabilized 486-nm reference laser. The frequency of this second-harmonic radiation is compared with that of the 243-nm sum-frequency synthesizer output by mixing the two beams on a photomultiplier. The generated beat signal is monitored with an rf spectrum analyzer. We use the spectrum analyzer in the zero-frequency span mode so that it acts merely as a tuned receiver. In this configuration, the spectrum analyzer output displays a resonance peak whenever the beat frequency is scanned through the frequency to which the spectrum analyzer is tuned. As we scan the frequency of the 243-nm radiation over the hydrogen 1S-2S resonance, we discretely change the frequency of the spectrum analyzer so as to record several “beat note” resonances. We thus obtain a series of peaks that resembles the output of a Fabry-Pérot étalon, though here we have absolute as well as relative frequency information.

IV. MEASUREMENT

During this experiment we have recorded and evaluated several hundred spectra in order to reduce statistical uncertainties and to determine systematic corrections. Figure 3 shows a representative spectrum of the $F=1$ component of the hydrogen 1S-2S transition, obtained by scanning the frequency of the 790-nm dye laser. For this particular trace the cell contained 0.225 Torr of atomic and molecular hydrogen, the circulating 243-nm intensity was 65 W/cm^2 at the beam waist, and the peak excitation rate was 4000 s^{-1} with a signal-to-background ratio of 20:1. As described above, the “marker fringes” shown in Fig. 3 are obtained from the heterodyne comparison with the second harmonic of the 486-nm reference laser.

We determine the line center of the $F=1$ component of the hydrogen 1S-2S transition by fitting the recorded signal²⁹ to a Lorentzian line shape. The quality of our

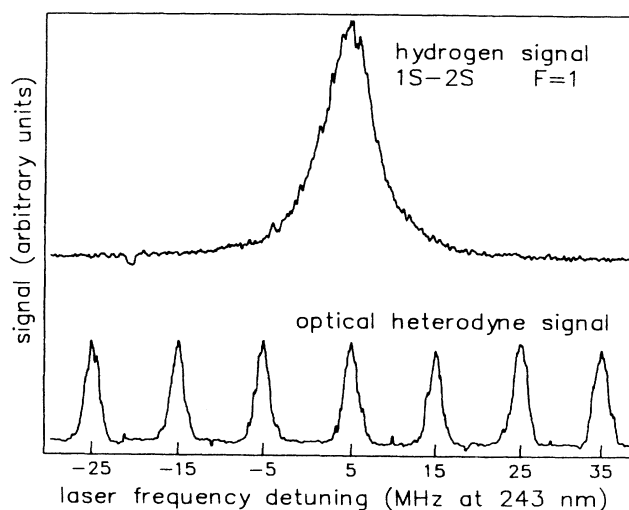


FIG. 3. Continuous-wave two-photon spectrum of the $F=1$ component of the hydrogen 1S-2S transition. The peaks in the simultaneously recorded spectrum analyzer output are described in the text. The laser frequency detuning is with respect to the second harmonic of the 486-nm reference laser.

fitting procedure is limited by both the 1S-2S signal-to-noise ratio and small nonlinearities in the scan rate of the 790-nm fundamental laser frequency. By observing the response of χ^2 to small variations in the fit parameters, we estimate the uncertainty in our ability to identify the line center to be 185 kHz (at 243 nm). We determine the center of each heterodyne signal maximum simply as the center of gravity of the top half of the peak.

There are two potentially significant sources of systematic error in this experiment, in addition to pressure broadening and shifting of the line shape: the second-order Doppler shift and the dc Stark shift. The second-order Doppler effect has an estimated value of -34 kHz; as this is not a significant correction, we include it only as a small systematic uncertainty. We estimate that the nearby cathode of the Lyman- α photomultiplier may generate a dc electric field as large as 6 V/cm at the interaction region. This is the most significant source of possible electric fields and would produce a dc Stark shift of 65 kHz at 243 nm. If we include the second-order Doppler shift and the dc Stark shift in our line center uncertainty, then it increases to 200 kHz. We add this error in quadrature to the statistical errors obtained from the fits and the subsequent averaging procedure.

Here we briefly consider the possible effects of the ac Stark shift. The ac Stark shift of the resonance frequency ω_{ab} is given by

$$\Delta\omega_{acS} = \frac{1}{\pi^2 \hbar c} \left[\frac{\alpha}{2R_\infty} \right]^3 M_{acS} I, \quad (1)$$

where α is the fine-structure constant, R_∞ is the Rydberg constant, I is the circulating intensity, and M_{acS} is a dimensionless two-photon amplitude.^{4,30} We have computed M_{acS} for the hydrogen 1S-2S transition using the matrix elements listed by Lee.³¹ In Ref. 31 the contribution due to virtual intermediate transitions from the 2S state to the continuum was underestimated due to an improper treatment of a pole in the integrand.³² By employing the principal-value algorithm

$$P \int_0^\infty dx \frac{f(x)}{x-c} \simeq \int_0^{c-\epsilon} dx \frac{f(x)}{x-c} + \int_{c-\epsilon}^\infty dx \frac{f(x)}{x-c} + 2\epsilon f'(c) + O[\epsilon^2 f''(c)], \quad (2)$$

for small ϵ , and by carefully estimating remainders after truncation of both series and integrals, we obtain the discrete and continuum contributions to M_{acS} listed in Table IV. The error in each entry in the table is less than 1 in the last digit. We obtain $M_{acS} = 53.35$, and therefore the total ac Stark shift of the 1S-2S transition is (at 243 nm)

TABLE IV. ac Stark shift of the H 1S-2S transition: contributions to M_{acS} .

State	Discrete	Continuum	Total
1S	-7.187 07	-1.384 09	-8.571 16
2S	34.793 68	9.986 63	44.780 32
2S-1S	41.980 75	11.370 72	53.351 47

$$\begin{aligned} \Delta f_{acS}(1S-2S) &= \frac{\Delta\omega_{acS}(1S-2S)}{4\pi} \\ &= 1.667I \text{ Hz W}^{-1} \text{ cm}^2. \end{aligned} \quad (3)$$

For the intensities used in this experiment ($\simeq 50 \text{ W/cm}^2$), this effect can thus be neglected.

V. RESULTS

The observed pressure broadening of the $F=1$ component of the hydrogen 1S-2S transition is displayed in Fig. 4. Fits to the data yield broadenings of 15.1(6) MHz/Torr (at 243 nm) for 100% H_2 and 9.2(5) MHz/Torr (at 243 nm) for the 0.7% H_2 -99.3% He mixture. The resulting zero-pressure linewidth, limited by the linewidths of the fundamental lasers and by transit-time broadening, is 3.7(3) MHz.

Figure 5 displays the frequency offset (at 243 nm) of the $F=1$ component of the hydrogen 1S-2S transition relative to the second harmonic of the 486-nm reference laser frequency as a function of total cell pressure for the two data sets. The weighted linear least-squares fits to the data are also shown and yield pressure shifts of $-5.52(48)$ MHz/Torr for the pure H_2 data set and $-0.65(33)$ MHz/Torr for the 0.7% H_2 -99.3% He data. However, in the pure H_2 case, it is unclear whether the hydrogen atoms or molecules are more responsible for the perturbation. This is troubling in light of the uncertainty of the gas composition as a function of pressure. Observation of the discharge color and of the resistance of a semiconductor detector downstream of the discharge⁴ suggests that the ratio of atoms to molecules changes with pressure for the pure H_2 data set. This ratio is more consistent for the 0.7% H_2 -99.3% He mixture data, and is also less important because of the large percentage of He atoms. Thus, we feel less justified in fitting the pure H_2 data to a straight line and must rely on the 0.7% H_2 -99.3% He mixture to determine the frequency offset without the pressure shift.

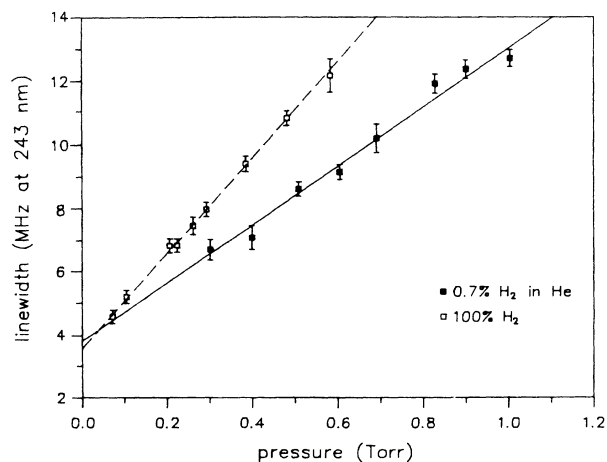


FIG. 4. Pressure broadening of the hydrogen 1S-2S $F=1$ resonance line. The displayed lines are the best-weighted fits to the corresponding data sets.

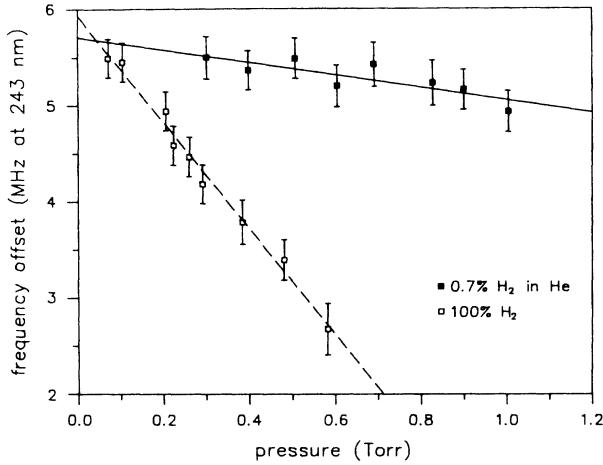


FIG. 5. Pressure shift of the hydrogen 1S-2S $F=1$ resonance line. The displayed lines are the best-weighted fits to the corresponding data sets.

The measured cell pressure includes 0.04(1) Torr of background pressure due to a leak in our vacuum system. The 0.7% H_2 -99.3% He data thus should be extrapolated to 0.04 Torr, rather than to zero, and then corrected for the pressure shift due to 0.04 Torr of air. Unfortunately, this shift is not known, so we must account for that uncertainty. To estimate this, we assume that the background gas is mostly N_2 , that the pressure shift in the pure H_2 data is due to H_2 (as opposed to H atoms), and that N_2 and H_2 have similar shifts. This last point is somewhat justified by the fact that N_2 has a 50% larger cross section than H_2 for quenching of H(2S) metastable atoms.³³ The measured shift of 0.04 Torr of H_2 (from above) is 0.22 MHz. We therefore estimate the uncertainty caused by the background gas as 0.33 MHz. We add this uncertainty to that of the extrapolated value and obtain the result shown in Table V.

Finally, we must add $\frac{1}{4}$ of the difference between the

experimental values of 1S and 2S hyperfine splittings^{34,35} to the observed frequency of the $F=1$ component (at 121.6 nm) to arrive at an experimental value for the centroid of the 1S-2S energy interval. The resultant experimental 1S-2S centroid frequency is shown in Table V as

$$f(1S-2S) = 2\,466\,061\,413.19(175) \text{ MHz} . \quad (4)$$

VI. COMPARISON WITH THEORY

For a comparison with theory, we adopt the conventions and update the results of Johnson and Soff,³ including the recent radiative recoil corrections of Bhatt and Grotch,³⁶ and the pure recoil corrections of Erickson and Grotch,³⁷ as well as more precise computations and error estimates.³⁸ The energy levels of a one-electron atom may be written as the sum of a Dirac-Coulomb contribution $E_{\text{DC}}(n, J)$ a reduced-mass correction $E_{\text{RM}}(n, J)$, the Lamb shift $E_{\text{LS}}(n, J, L)$, and a hyperfine-structure contribution $E_{\text{HFS}}(n, J, L, F, I)$:

$$E(n, J, L, F, I) = E_{\text{DC}}(n, J) + E_{\text{RM}}(n, J) + E_{\text{LS}}(n, J, L) + E_{\text{HFS}}(n, J, L, F, I) , \quad (5)$$

where n is the principal quantum number, J is the total momentum of the electron, L is the orbital angular momentum of the electron, F is the total atomic angular momentum, and I is the spin of the nucleus. We express all energies in units of Hz.

As defined by Johnson and Soff,³ the Lamb shift includes QED radiative and binding contributions, relativistic radiative and nonradiative nuclear recoil corrections, and corrections due to the nonzero rms charge radius of the nucleus. We write the total Lamb shift in the form

$$E_{\text{LS}}(n, J, L) = \frac{2}{\pi\alpha} \frac{(Z\alpha)^4}{n^3} cR_{\infty} F(Z\alpha) , \quad (6)$$

where $2\alpha^3 cR_{\infty} / \pi = \alpha^5 m_e c^2 / \pi h = 813.862\,88(11) \text{ MHz}$.

TABLE V. Determination of the hydrogen 1S-2S centroid frequency.

	Frequency (MHz)	Error ^a (MHz)
486.3 nm		
Stabilized laser frequency		
f_{ref}	616 515 272.78	0.39
243.1 nm		
Hydrogen ($F=1$) offset ^b		
$f_{\text{H}_1} - 2f_{\text{ref}}$	5.68	0.40
121.6 nm		
Hydrogen hyperfine splitting ^c		
$\Delta f_{\text{hfs}}(1S-2S) = \frac{1}{4} [\Delta f_{\text{hfs}}(1S) - \Delta f_{\text{hfs}}(2S)]$	310.71	0.00
Hydrogen 1S-2S centroid		
$f(1S-2S) = 2f_{\text{H}_1} + \Delta f_{\text{hfs}}(1S-2S)$	2 466 061 413.19	1.75

^aOne standard deviation.

^b $f_{\text{H}_1} = \frac{1}{2} f(1S-2S)_{F=1}$.

^cReferences 35 and 36.

TABLE VI. Contributions to the Lamb-shift function $F(Z\alpha)$ for hydrogen 1S and 2S states.

Term	1S	2S
Self-energy	10.316 76(10)	10.546 83(10)
Vacuum polarization	-0.264 38	-0.264 39
Higher-order QED	0.001 25(1)	0.001 25(1)
Relativistic reduced mass	-0.015 71	-0.016 09
Relativistic recoil	0.002 93(3)	0.003 33(3)
Finite nuclear size	0.001 25(3)	0.001 25(3)
Total $F(Z\alpha)$	10.042 10(11)	10.272 18(11)

The contributions to $F(Z\alpha)$ are shown in Table VI for the 1S and 2S states of hydrogen. These values and uncertainties have been updated³⁶⁻³⁸ since their original publication.³ The total energies of the 1S and 2S states are shown in Table VII, as well as the fundamental constants used in the computations.^{26,39-42} We have adopted the rms charge radius of the proton given by Ref. 42 instead of the slightly larger value of Ref. 43. Use of the latter would raise the theoretical 1S Lamb shift by 0.15 MHz. This discrepancy is larger than the theoretical uncertainty and, unless resolved, will limit the ability of future measurements to test QED.

Table VIII shows the steps required to determine the hydrogen 1S Lamb shift using the experimental value of the 1S-2S transition frequency given by Eq. (4). We begin by summing the theoretical Dirac Coulomb and reduced mass contributions, given in Table VII, and then subtracting the experimental 1S-2S transition frequency to obtain the difference between the 1S and 2S Lamb shifts, $f_{LS}(1S) - f_{LS}(2S) = 7128.85(188)$ MHz. We add to this number the experimentally known $2S_{1/2} - 2P_{1/2}$ frequency separation; because of their small errors, either the value measured by Lundeen and Pipkin,¹ 1057.845(9) MHz, or by Pal'chikov, Sokolov, and Yaklovev,² 1057.8514(19), may be used without affecting our result. Finally, we can

TABLE VII. Hydrogen 1S and 2S energy levels and transition frequencies (in MHz). The following values of fundamental constants were used: $c = 299\,792\,458$ m/s (Ref. 26), $R_\infty = 109\,737.315\,73(3)$ cm⁻¹ (Ref. 39), $\alpha = 1/137.035\,989\,5(61)$ (Ref. 40), $m_p/m_e = 1836.152\,701(37)$ (Ref. 41), and $r_p = 0.805(11)$ fm (Ref. 42).

Term	Value
1S	
Dirac energy	-3 289 885 760.01(90)
Reduced mass	1 790 728.67(04)
Lamb shift	8172.89(09)
Total energy	-3 288 086 858.45(91)
2S	
Dirac energy	-822 474 177.42(22)
Reduced mass	447 688.12(01)
Lamb shift	1045.02(01)
Total energy	-822 025 444.28(22)
$f(1S-2S)$	2 466 061 414.17(68)

confidently add the theoretical $2P_{1/2}$ Lamb shift,^{3,4} $f_{LS}(2P) = -12.8299(3)$ MHz, to obtain the ground-state Lamb shift

$$f_{LS}(1S) = 8173.9(19) \text{ MHz} , \quad (7)$$

in good agreement with the theoretical prediction of 8172.89(9) MHz shown in Table VII. In Table IX we compare our result with those of previous experiments^{5-7,44} as well as the subsequent experiment of Boshier *et al.*⁴⁵ We have updated the measurements of Ref. 6 to conform to the reduced mass convention of Johnson and Soff.³

This procedure may be summarized by a simple formula that includes the Rydberg constant as a parameter:

$$f_{LS}(1S) = 8172.39 \text{ MHz} + (224.7 \text{ MHz m}) \times (R_\infty - 10\,973\,731.57 \text{ m}^{-1}) + [2\,466\,061\,414 \text{ MHz} - f(1S-2S)] . \quad (8)$$

The corresponding one-sigma error in $f_{LS}(1S)$ can be found in terms of the experimental uncertainties in $f(1S-2S)$ and R_∞ from the expression

$$\Delta f_{LS}^2(1S-2S) = \Delta f^2(1S-2S) + (224.7 \text{ MHz m})^2 \Delta R_\infty^2 . \quad (9)$$

On the other hand, if we trust the theoretical determination of the 1S Lamb shift, then we can interpret our experimental result as a measurement of the Rydberg

TABLE VIII. Determination of experimental hydrogen 1S Lamb shift.

Term	Value (MHz)	Error ^a (MHz)
$f_{\text{Dirac}}(1S-2S)$	2 467 411 582.59	0.68
$f_{\text{RM}}(1S-2S)$	-1 343 040.55	0.03
$-f(1S-2S)$	-2 466 061 413.19	1.75
$f_{LS}(1S) - f_{LS}(2S)$	7128.85	1.88
$f_{LS}(2S) - f_{LS}(2P)^b$	1057.85	0.01
$f_{LS}(2P)^c$	-12.83	0.00
$f_{LS}(1S)$	8173.87	1.88

^aOne standard deviation.

^bReferences 1 and 2.

^cReferences 3 and 4.

TABLE IX. Measurements of the hydrogen 1S Lamb shift.

Reference	Isotope	$\Delta f_{\text{Lamb}}(1S)$ (in MHz)
Herzberg ^a	D	7900(1100)
Hänsch <i>et al.</i> ^b	D	8300(300)
Lee <i>et al.</i> ^c	D	8260(110)
Wieman and Hänsch ^d	D	8189(30)
Boshier <i>et al.</i> ^e	D	8183.96(80)
Hänsch <i>et al.</i> ^b	H	8600(800)
Lee <i>et al.</i> ^c	H	8220(100)
Wieman and Hänsch ^d	H	8175(30)
Hildum <i>et al.</i> ^f	H	8184.8(54)
This work	H	8173.9(19)
Boshier <i>et al.</i> ^e	H	8172.93(84)

^aReference 44.^bReference 5.^cReference 6.^dReference 7.^eReference 45.^fReference 8.

constant. By solving Eqs. (8) and (9) for R_∞ and ΔR_∞ , respectively, with $f_{1S}(1S) = 8172.89(9)$, we obtain

$$R_\infty = 10\,973\,731.57 \text{ m}^{-1} + \frac{f(1S-2S) - 2\,466\,061\,413.50 \text{ MHz}}{224.7 \text{ MHz m}}, \quad (10)$$

$$\Delta R_\infty^2 = \frac{\Delta f^2(1S-2S) + (0.09 \text{ MHz})^2}{(224.7 \text{ MHz m})^2}. \quad (11)$$

For $f(1S-2S)$ given by Eq. (4), we have

$$R_\infty = 109\,737.315\,69(8) \text{ cm}^{-1}, \quad (12)$$

as shown in Table X, in good agreement with the most recent measurements.^{39,45-47}

VII. CONCLUSION

In summary, we have measured the absolute frequency of the hydrogen 1S-2S transition with a precision of 7 parts in 10^{10} using continuous-wave Doppler-free two-photon spectroscopy. As a result, we have determined the hydrogen 1S Lamb shift with an uncertainty of 2 parts in 10^4 . This error is limited primarily by the $^{130}\text{Te}_2$ frequency reference and secondarily by pressure shift un-

TABLE X. Recent laser measurements of the Rydberg constant.

Reference	Transition	$R_\infty - 109\,737 \text{ cm}^{-1}$
Zhao <i>et al.</i> ^a	H,D 2S-3P	0.315 69(7)
Biraben <i>et al.</i> ^b	H,D 2S-8D,10D	0.315 69(6)
Zhao <i>et al.</i> ^c	H,D 2S-4P	0.315 73(3)
This work	H 1S-2S	0.315 69(8)
Boshier <i>et al.</i> ^d	H,D 1S-2S	0.315 73(3)

^aReference 46.^bReference 47.^cReference 39.^dReference 45.

certainties in the cell. The frequency reference limitation can be surpassed by employing a frequency chain that takes advantage of the near coincidence between the seventh harmonic of a 3.39- μm CH_4 stabilized He-Ne laser and the 486-nm light used above. The pressure shift problem is more easily overcome through the use of a hydrogen beam. Unfortunately, the current experimental uncertainty in the Rydberg constant³⁹ means that an absolute frequency measurement cannot determine the 1S Lamb shift to better than 675 kHz. However, direct comparison with other narrow transitions in hydrogen can overcome this limitation. In particular, the two-photon 2S- nD transitions (for $n=8, 10$, and 12) have recently been measured⁴⁸ with a precision of 4.3 parts in 10^{-11} (and an absolute accuracy of 1.7 parts in 10^{-10}). Comparison with the 1S-2S transition would allow a determination of the 1S Lamb shift to 100 kHz.

ACKNOWLEDGMENTS

We are grateful to W. R. Johnson, J. Sapirstein, and H. Grotch for many illuminating discussions and to J. L. Hall for the loan of some valuable equipment and for his expert advice. We thank P. J. Gardner, J. L. Cannon, and other staff members of Coherent, Inc., for their skilled assistance with various components of this experiment. One of the authors (D.H.M.) acknowledges support from the National Science Foundation. This work was supported in part by the National Science Foundation under Grant No. NSF PHY86-04441 and by the U.S. Office of Naval Research under Contract No. ONR N00014-C-78-0403.

*Present address: Max-Planck-Institut für Quantenoptik, D-8046 Garching, Federal Republic of Germany.

†Permanent address: Boeing High Technology Center, P.O. Box 24969, MS 7J-05, Seattle, WA 98124-6269.

‡Permanent address: Clarendon Laboratory, Parks Road, Oxford OX1 3PU, England.

§Permanent address: Lawrence Livermore National Laboratory, Livermore, CA 94550.

**Permanent address: Coherent, Inc., Palo Alto, CA 94303.

††Permanent address: Max-Planck-Institut für Quantenoptik, D-8046 Garching, and Sektion Physik, University of Munich, 8000 Munich 40, Federal Republic of Germany.

‡‡S. R. Lundeen and F. M. Pipkin, Phys. Rev. Lett. **46**, 232

(1981).

²V. G. Pal'chikov, Yu. L. Sokolov, and V. P. Yakovlev, Metrologia **21**, 99 (1985).

³W. R. Johnson and G. Soff, At. Data Nucl. Data Tables **33**, 405 (1985).

⁴R. G. Beausoleil, Ph.D. dissertation, Stanford University, 1986.

⁵T. W. Hänsch, S. A. Lee, R. Wallenstein, and C. Weiman, Phys. Rev. Lett. **34**, 307 (1975).

⁶S. A. Lee, R. Wallenstein, and T. W. Hänsch, Phys. Rev. Lett. **35**, 1262 (1975).

⁷C. E. Wieman and T. W. Hänsch, Phys. Rev. A **22**, 192 (1980).

⁸E. A. Hildum, U. Boesl, D. H. McIntyre, R. G. Beausoleil, and T. W. Hänsch, Phys. Rev. Lett. **56**, 576 (1986).

- ⁹J. R. M. Barr, J. M. Girkin, J. M. Tolchard, and A. I. Ferguson, *Phys. Rev. Lett.* **56**, 580 (1986).
- ¹⁰C. J. Foot, B. Couillaud, R. G. Beausoleil, and T. W. Hänsch, *Phys. Rev. Lett.* **54**, 1913 (1985).
- ¹¹R. G. Beausoleil, D. H. McIntyre, C. J. Foot, E. A. Hildum, B. Couillaud, and T. W. Hänsch, *Phys. Rev. A* **35**, 4878 (1987).
- ¹²T. W. Hänsch and B. Couillaud, *Opt. Commun.* **35**, 441 (1980).
- ¹³B. Couillaud, T. W. Hänsch, and S. G. McLean, *Opt. Commun.* **50**, 127 (1984).
- ¹⁴M. Brieger, H. Büsener, A. Hese, F. v. Moers, and A. Renn, *Opt. Commun.* **38**, 423 (1981).
- ¹⁵N. Wang and U. Gaubatz, *Appl. Phys. B* **40**, 43 (1986).
- ¹⁶H. W. Kogelnik, E. P. Ippen, A. Dienes, and C. V. Shank, *IEEE J. Quantum Electron.* **QE-8**, 373 (1972).
- ¹⁷H. Kogelnik and T. Li, *Appl. Opt.* **5**, 1550 (1966).
- ¹⁸R. A. Phillips, *J. Opt. Soc. Am.* **56**, 629 (1966); M. Yamazaki and T. Ogawa, *ibid.* **56**, 1407 (1966).
- ¹⁹G. D. Boyd and D. A. Kleinman, *J. Appl. Phys.* **39**, 3597 (1968).
- ²⁰J. Cariou and P. Luc, *Atlas du Spectre d'Absorption de la Molecule de Tellure* (Laboratoire Aime-Cotton, CNRS, Orsay, France, 1980).
- ²¹R. E. Machol and E. F. Westrum, Jr., *J. Am. Chem. Soc.* **80**, 2950 (1958).
- ²²J. R. M. Barr, J. M. Girkin, A. I. Ferguson, G. P. Barwood, P. Gill, W. R. C. Rowley, and R. C. Thompson, *Opt. Commun.* **54**, 217 (1985).
- ²³D. H. McIntyre and T. W. Hänsch, *Phys. Rev. A* **34**, 4504 (1986).
- ²⁴D. H. McIntyre and T. W. Hänsch, *Phys. Rev. A* **36**, 4115 (1987).
- ²⁵D. H. McIntyre, Ph.D. dissertation, Stanford University, 1987.
- ²⁶See the documents concerning the new definition of the meter, *Metrologia* **19**, 163 (1984).
- ²⁷G. C. Bjorklund, *Opt. Lett.* **5**, 15 (1980).
- ²⁸J. L. Hall, L. Hollberg, T. Baer, and H. G. Robinson, *Appl. Phys. Lett.* **39**, 680 (1981).
- ²⁹E. A. Hildum, Ph.D. dissertation, Stanford University, 1986.
- ³⁰R. G. Beausoleil and T. W. Hänsch, *Phys. Rev. A* **33**, 1661 (1986).
- ³¹S. A. Lee, Ph.D. dissertation, Stanford University, 1975.
- ³²S. Chu (private communication).
- ³³S. R. Ryan, S. J. Czuchlewski, and M. V. McCusker, *Phys. Rev. A* **16**, 1892 (1973).
- ³⁴P. Petit, M. Desaintfuscien, and C. Audoin, *Metrologia* **16**, 7 (1980).
- ³⁵J. W. Heberle, H. A. Reich, and P. Kusch, *Phys. Rev.* **101**, 612 (1956).
- ³⁶G. Bhatt and H. Grotch, *Phys. Rev. A* **31**, 2794 (1985); *Phys. Rev. Lett.* **58**, 471 (1987).
- ³⁷G. W. Erickson and H. Grotch, *Phys. Rev. Lett.* **60**, 2611 (1988).
- ³⁸W. R. Johnson (private communication).
- ³⁹P. Zhao, W. Lichten, H. Layer, and J. Bergquist, *Phys. Rev. Lett.* **58**, 1293 (1987).
- ⁴⁰E. R. Cohen and B. N. Taylor, *CODATA Bull.* **63**, 1 (1986) [reprinted in *Rev. Mod. Phys.* **59**, 1121 (1987)].
- ⁴¹R. S. Van Dyck, Jr., F. L. Moore, D. L. Farnham, and P. B. Schwinberg, *Bull. Am. Phys. Soc.* **31**, 224 (1986).
- ⁴²L. N. Hand, D. J. Miller, and R. Wilson, *Rev. Mod. Phys.* **35**, 335 (1963).
- ⁴³G. G. Simon, Ch. Schmitt, F. Borkowski, and V. H. Walther, *Nucl. Phys. A* **333**, 381 (1980).
- ⁴⁴G. Herzberg, *Proc. R. Soc. London, Ser. A* **234**, 516 (1956).
- ⁴⁵M. G. Boshier, P. E. G. Baird, C. J. Foot, E. A. Hinds, M. D. Plimmer, D. N. Stacey, J. B. Swan, D. A. Tate, D. M. Warrington, and G. K. Woodgate, *Nature* **330**, 463-465 (1987).
- ⁴⁶P. Zhao, W. Lichten, H. P. Layer, and J. C. Bergquist, *Phys. Rev. A* **34**, 5138 (1986).
- ⁴⁷F. Biraben, J. C. Garreau, and L. Julien, *Europhys. Lett.* **2**, 925 (1986).
- ⁴⁸F. Biraben, J. C. Garreau, L. Julien, and M. Allegrini, *Phys. Rev. Lett.* **62**, 621 (1989).